

RESEARCH

Open Access



Exploring the mechanism of 6-Methoxydihydrosanguinarine in the treatment of lung adenocarcinoma based on network pharmacology, molecular docking and experimental investigation

Xingyun Liu¹, Yanling Ren^{2,4}, Shuanglin Qin^{3*} and Zerui Yang^{2,4*}

Abstract

Background 6-Methoxydihydrosanguinarine (6-MDS) has shown promising potential in fighting against a variety of malignancies. Yet, its anti-lung adenocarcinoma (LUAD) effect and the underlying mechanism remain largely unexplored. This study sought to explore the targets and the probable mechanism of 6-MDS in LUAD through network pharmacology and experimental validation.

Methods The proliferative activity of human LUAD cell line A549 was evaluated by Cell Counting Kit-8 (CCK8) assay. LUAD related targets, potential targets of 6-MDS were obtained from databases. Venn plot analysis were performed on 6-MDS target genes and LUAD related genes to obtain potential target genes for 6-MDS treatment of LUAD. The Search Tool for the Retrieval of Interacting Genes/Proteins (STRING) database was utilized to perform a protein-protein interaction (PPI) analysis, which was then visualized by Cytoscape. The hub genes in the network were singled out by CytoHubba. Metascape was employed for GO and KEGG enrichment analyses. molecular docking was carried out using AutoDock Vina 4.2 software. Gene expression levels, overall survival of hub genes were validated by the GEPIA database. Protein expression levels, promotor methylation levels of hub genes were confirmed by the UALCAN database. Timer database was used for evaluating the association between the expression of hub genes and the abundance of infiltrating immune cells. Furthermore, correlation analysis of hub genes expression with immune subtypes of LUAD were performed by using the TISIDB database. Finally, the results of network pharmacology analysis were validated by qPCR.

Results Experiments in vitro revealed that 6-MDS significantly reduced tumor growth. A total of 33 potential targets of 6-MDS in LUAD were obtained by crossing the LUAD related targets with 6-MDS targets. Utilizing CytoHubba, a network analysis tool, the top 10 genes with the highest centrality measures were pinpointed, including MMP9, CDK1,

*Correspondence:

Shuanglin Qin
shuanglin@tju.edu.cn
Zerui Yang
yzz_gzucm1991@163.com

Full list of author information is available at the end of the article



© The Author(s) 2024. **Open Access** This article is licensed under a Creative Commons Attribution 4.0 International License, which permits use, sharing, adaptation, distribution and reproduction in any medium or format, as long as you give appropriate credit to the original author(s) and the source, provide a link to the Creative Commons licence, and indicate if changes were made. The images or other third party material in this article are included in the article's Creative Commons licence, unless indicated otherwise in a credit line to the material. If material is not included in the article's Creative Commons licence and your intended use is not permitted by statutory regulation or exceeds the permitted use, you will need to obtain permission directly from the copyright holder. To view a copy of this licence, visit <http://creativecommons.org/licenses/by/4.0/>. The Creative Commons Public Domain Dedication waiver (<http://creativecommons.org/publicdomain/zero/1.0/>) applies to the data made available in this article, unless otherwise stated in a credit line to the data.

TYMS, CCNA2, ERBB2, CHEK1, KIF11, AURKB, PLK1 and TTK. Analysis of KEGG enrichment hinted that these 10 hub genes were located in the cell cycle signaling pathway, suggesting that 6-MDS may mainly inhibit the occurrence of LUAD by affecting the cell cycle. Molecular docking analysis revealed that the binding energies between 6-MDS and the hub proteins were all higher than -6 kcal/Mol with the exception of AURKB, indicating that the 9 targets had strong binding ability with 6-MDS. These results were corroborated through assessments of mRNA expression levels, protein expression levels, overall survival analysis, promoter methylation level, immune subtypes and immune infiltration. Furthermore, qPCR results indicated that 6-MDS can significantly decrease the mRNA levels of CDK1, CHEK1, KIF11, PLK1 and TTK.

Conclusions According to our findings, it appears that 6-MDS could possibly serve as a promising option for the treatment of LUAD. Further investigations in live animal models are necessary to confirm its potential in fighting cancer and to delve into the mechanisms at play.

Keywords 6-Methoxydihydroanguinarine, Lung adenocarcinoma, Network pharmacology, Molecular docking

Introduction

Lung cancer, composed of approximately 85% non-small-cell lung cancer (NSCLC) and 15% small cell lung cancer (SCLC), is one of the most prevalent malignant cancers worldwide, with over 1.4 million deaths each year [1]. According to Global cancer statistics 2022 published in 2024, with almost 2.5 million new cases and over 1.8 million deaths worldwide, lung cancer is the leading cause of cancer morbidity and mortality in 2022 [2]. Another study estimates that there will be 3.8 million incident cases and 3.2 million deaths globally due to lung cancer in 2050 [3]. To date, Lung adenocarcinoma (LUAD) is the most common subtype of NSCLC [4, 5]. Despite improvements in chemotherapy, radiotherapy, and surgery, the prognosis of NSCLC still remains poor, and the five-year survival rate is only approximately 18% [6]. Patients with advanced-stage disease are treated with chemotherapeutic medications such as platinum [7]. However, the development of resistance to chemotherapeutic medications and the occurrence of adverse responses to these treatments have become major challenges in modern oncology [8]. The mechanisms underlying resistance to chemotherapeutic medications are multifactorial. It has been reported that cisplatin resistance often occurs due to a cellular defense mechanism that confers resistance by reducing the ability to mediate apoptosis, enhancing the repair of DNA damage, altering cell cycle checkpoints, and disrupting cytoskeleton assembly [9]. Nevertheless, the exact mechanisms of resistance to chemotherapeutic medications remain largely unclear [10]. Meanwhile, targeted therapy and immunotherapy have been developed to overcome these problems, but it has faced acquired resistance, poor therapeutic response, systemic immune dysfunction [11, 12]. The clinical outcomes and effects of neoadjuvant therapy (including Chemotherapy/Radiotherapy, Targeted Therapy and Immunotherapy) for NSCLC are still controversial due to its apparent advantages and disadvantages [13]. Considering the existing controversy concerning the efficacy of current therapy

for patients with NSCLC, searching for low toxicity and effective anti-cancer drugs and new drug targets has been a research direction in recent years.

Traditional Chinese medicine (TCM) has long been utilized as a complementary treatment for various types of cancer, such as lung cancer [14]. TCM is characterized by the utilization of medicines derived from natural herbs, rather than being created through chemical synthesis [15]. These herbal drugs have low toxicity and exert complex anti-cancer effects through a variety of intricate mechanisms [16]. Therefore, the active ingredients extracted from Chinese herbs have become a hot spot for global research [17]. *Macleaya cordata* (Chinese name “Bo-luo-hui”) is a perennial herb that belongs to the Papaveraceae family and is typically prescribed as a traditional antibacterial medicine, whose effect and usage were well documented in Ben-Cao-Shi-Yi, a Chinese encyclopedia of botany and medicine from the early Tang dynasty [18]. According to literature, it has significant therapeutic effects on ulcers, snake and insect bites, anti-tumor effects, and improving liver function [19]. The main component of *Macleaya cordata* extract is alkaloid. More than 70 kinds of alkaloids have been reported to be isolated and identified from *Macleaya cordata*, and 6-Methoxydihydroanguinarine (6-MDS) belongs to one of the isoquinoline alkaloids. It is reported that 6-MDS has antimicrobial activity and has significant inhibitory activity against *Staphylococcus aureus* [20]. In addition, 6-MDS can induce proliferation and apoptosis of HT29 cells and Hep G2 cells, with IC_{50} values of 3.8 ± 0.2 and 5.0 ± 0.2 μ M, respectively [21, 22]. The latest research showed that 6-MDS can induce apoptosis and autophagy of breast cancer MCF-7 cells by inhibiting PI3K/AKT/mTOR signaling pathway by accumulating ROS, which has great potential in the treatment of cancer [20]. Also, 6-MDS exhibits cytotoxicity and sensitizes TRAIL-induced apoptosis of hepatocellular carcinoma cells through ROS-mediated upregulation of DR5 [23].

However, its anti-LUAD effect and its mechanism have not yet been reported.

Traditional studies often focus on a single gene or target, ignoring the complexity and systematicness of biological processes. However, Chinese medicine has multi-target and multi-pathway mechanisms of action for treating diseases. Therefore, it is necessary to use big data to mine all existing targets and pathways related to 6-MDS and LUAD. In recent years, the network pharmacology has developed, which integrates the system biology and pharmacology, integrates the biological network and pharmacology, changes the traditional search for a single target to comprehensive network analysis, emphasizes the interaction mode of multicomponents, multi-targets, and multipathways, and is especially suitable for predicting the action target and possible mechanism of natural compounds from traditional Chinese medicines or different plants [24, 25]. In the present study, our team used the network pharmacology technique and in vitro experiment to access the molecular pathways behind 6-MDS's ability to block LUAD proliferation.

Methods

Cell experiment verification

Cell culture

A549 cells were purchased from American Type Culture Collection (ATCC, Manassas, VA) and were cultured in RPMI 1640 medium (CT1875500BT, Gibco, ThermoFisher Scientific, USA) supplemented with 10% fetal bovine serum (164210-50, FBS, Procell, Wuhan, Hubei, China) plus penicillin G (15140-122, Gibco, ThermoFisher Scientific, USA, 100 U/mL) and streptomycin (15140-122, Gibco, ThermoFisher Scientific, USA, 100 U/mL) at 37 °C under 5% CO₂ [26].

Cell viability assays

Cells were inoculated into 96-well flat-bottomed microtiter plates with 6000 cells per well, after 24 h of cultivation, they were treated with 6-MDS for 24 h and 48 h, respectively. Then, on the basis of the manufacturer's instructions, Cell Counting Kit-8 (CCK8, GK10001, Gp-Bio, USA) stock solution was added to each well and the plate was incubated in a cell culture incubator at 37 °C for 60 min. The absorbance at 450 nm was measured using a microplate reader (Multiskan-GO, Thermo Fisher Scientific, USA) to assess the cell viability [27].

Screening gene targets related to 6-MDS

First, the 2D, 3D structure, SDF file or SMILES of 6-MDS was downloaded from the PubChem website (<https://pubchem.ncbi.nlm.nih.gov/>) [28] and was then imported into the PharmMapper (Version 2017, <http://www.lilab-ecust.cn/pharmmapper/>) [29], SuperPred (Version 3.0, <https://prediction.charite.de/>) [30] SwissTargetPrediction

(Version2019, <http://swisstargetprediction.ch/>) [31] and targetnet (Version2016, <http://targetnet.scbdd.com/>) [32] for predicting the target genes. The parameters of PharmMapper were set as normalized fit score > 0.1. The cut-off of SwissTargetPrediction was set as probability > 0.1. The cut-off of targetnet was set as probability > 0.001 and the cut-off of SuperPred was set as probability > 0.5. After the target genes/proteins were obtained, the protein names were transformed to the corresponding gene names through the UniProt database (Release 2024_02, <http://www.uniprot.org>) [33] if necessary. Finally, the target genes obtained in the above four databases were combined to form a gene set.

LUAD-related target collection

The LUAD-related target genes were obtained in two ways. First, the differentially expressed genes (DEGs) specific to LUAD were acquired by extracting data from the GEPIA "Differential Expression Analysis" module by setting the parameter of |Log2FC| Cutoff: 1, q-value Cutoff: 0.01 (<http://gepia.cancer-pku.cn/detail.php?gene=&clicktag=expdiy>) [34]. Secondly, other potential targets associated with LUAD were identified through exploration three public database, which were OMIM (<https://www.omim.org/>) [35], Drugbank (version 6.0, <https://go.drugbank.com/>) [36], and GeneCards databases (Version 5.20, <https://www.genecards.org/>) [37] utilizing the search term "lung adenocarcinoma". Finally, potential LUAD-related targets were obtained by intersecting the DEGs extracted from the GEPIA database with the potential targets associated with LUAD sourced from the aforementioned trio of databases.

Determining the targets of 6-MDS in LUAD

For the identification of potential target genes for 6-MDS treatment of LUAD, an analysis using Venn diagrams was conducted on 6-MDS target genes and LUAD related genes. Subsequently, shared targets were found between 6-MDS target genes and LUAD related genes, which were considered as potential targets of 6-MDS in LUAD.

Enrichment analysis of the targets of 6-MDS in LUAD

Enrichment analysis of Gene Ontology (GO) and Kyoto Encyclopedia of Genes and Genomes (KEGG) were conducted using the online tool Metascape (Version 3.5.20240101, <https://metascape.org>) [38].

Protein-protein interaction (PPI) network construction and core targets screening

The STRING database (Version 12.0, <http://string-db.org/>) [39], which is an online database for evaluations of PPI, was employed to delve into the relationship between the proteins encoded by the potential targets of 6-MDS in LUAD. Subsequently, the results from STRING database

were exported to the plug-in CytoHubba of Cytoscape software (Version 3.9.0, <https://cytoscape.org/>) [40] to visualize the PPI network. Finally, maximal clique centrality (MCC) algorithm was performed to screen the top ten 10 genes, deemed as potential hub genes for subsequent investigation.

Molecular docking

Molecular docking is mainly used for the structural docking of small molecules with target proteins, and to evaluate their binding affinity with defined binding sites. It is generally believed that the lower the energy of the ligand receptor binding conformation, the more likely this effect is to occur [41]. Small molecule ligand files of chemical components were downloaded from the PubChem database, imported them into Chem3D software for the purpose of spatial structure transformation and energy optimization, and output them in mol 2 format file format. After processing with AutoDockTools 1.5.6 software, the files were saved in pdbqt format. Then the gene ID of the core target was retrieved from the Uniprot database and downloaded its corresponding PDB format file from the PDB database (<http://www.rcsb.org/>). After water molecule removal and ligand separation using PyMol software, the resultant macromolecular receptor file of the core target was imported into AutoDockTools 1.5.6 software for hydrogenation and saved in PDBqt format. Finally, with the help of AutoDockVina 1.1.2 software, the core target and its corresponding chemical components were molecularly docked, with the binding energy serving as the docking evaluation index. The predicted value of the dissociation constant (K_d) was calculated from $\Delta G = RT \ln(K_d)$ [42] where ΔG is the binding energy, R is the ideal gas constant ($\text{kcal} \cdot \text{K}^{-1} \cdot \text{mol}^{-1}$) and T is the temperature (K), with the help of an online web server developed by NovoPro Bioscience Inc. (<https://www.novoprolabs.com/tools/deltag2kd>).

External validation of hub genes

Gene expression analysis of hub genes

The GEPIA (<http://gepia.cancer-pku.cn/>) “Expression on Box Plots” and “Pathological Stage Plot” module were employed to explore the mRNA expression levels and pathological stages of the core targets in LUAD. A threshold of $|\log_2FC| \geq 1$ and a significance level of $p \leq 0.01$ were established for the analysis.

Protein expression analysis of core targets

UALCAN (<https://ualcan.path.uab.edu/>) [43] provides protein expression analysis option using data from Clinical Proteomic Tumor Analysis Consortium (CPTAC) and the International Cancer Proteogenome Consortium (ICPC) datasets [44]. Here, this database was utilized to conduct a comparative analysis of the protein expression

levels of the hub genes in LUAD tissues and their corresponding normal tissues.

Overall survival analysis of hub genes

Using the GEPIA database, the potential relationship between expression of the 9 hub genes and the OS of LUAD patients was evaluated by setting $p < 0.05$ as the criteria.

DNA methylation level of hub genes

The UALCAN database was used to compare DNA methylation level of hub genes between normal and LUAD tissues.

Correlation analysis of hub genes expression with immune cell infiltration

The online database TIMER (Version 2.0, <http://timer.cis-trome.org/>) [45] was utilized to analyze the correlation between the hub genes expression and infiltration score of B cell, CD4 T cell, CD8 T cell, neutrophil, macrophage and dendritic cell (DC).

Correlation analysis of core targets expression with immune and molecular subtypes of LUAD

The TISIDB database (<http://cis.hku.hk/TISIDB/index.php>) is an online integrated repository portal collecting abundant human cancer datasets sourced from the TCGA database [46]. The association between the expression level of core targets and immune or molecular subtypes of LUAD were assessed through the TISIDB database. Results were deemed statistically significant if the P-value was less than 0.05.

Real-time PCR validation

Primers and chemicals

Primers were purchased from Sangon Biotech (Shanghai, China). 6-MDS (WP23101106) was purchased from Sichuan Weikeqi Biological Technology Co. Ltd (Chengdu, Sichuan, China).

Real-time PCR

By using a SteadyPure Universal RNA Extraction Kit (AG21017, Accurate Biology, Hunan, China), total RNA of the cells was extracted. Subsequently, 1 μg of RNA was subjected to the reverse transcription process within a 20 μL reaction volume utilizing Evo M-MLVRT Mix Kit with gDNA Clean for qPCR Ver.2 (AG11728, Accurate Biology, Hunan, China). The resulting cDNA was then employed for real-time PCR assay by using the SYBR Green Pro Taq HS qPCR Kit (AG11701, Accurate Biology, Hunan, China). The specific primer sequences used in this study were as follows:

GAPDH-F: AAGGTGAAGGTCGGAGTCAA.

GAPDH-R: AATGAAGGGGTCATTGATGG.

CDK1-F: TAGGCGGGATCTACCATACCC.
 CDK1-R: TCATGGCTACCACTTGACCTG.
 CHEK1-F: CCAGATGCTCAGAGATTCTTCCA.
 CHEK1-R: TGTTCAACAAACGCTCACGATTA.
 KIF11-F: CGGAAAGCTAACGCCACTCAG.
 KIF11-R: TCTTATCAGCCAGTCCCTCCAGTTCG.
 PLK1-F: CACCAGCACGTCGTAGGATTC.
 PLK1-R: CCGTAGGTAGTATCGGGCCTC.
 TTK-F: AAACAGTGTTCGCTAAGTGATG.
 TTK-R: AGGGCAATTTCCAGCATTCTA.

Statistical analysis

GraphPad Prism 5.0 (GraphPad Software, San Diego, CA, USA; RRID: SCR_002798) was applied to analyzed the data. The analysis results of the data were presented in mean \pm SD. The statistical difference between two samples was analyzed by Students t test. * means $P < 0.05$, ** means $P < 0.01$ and *** means $P < 0.001$. P less than 0.05 indicates statistical difference in results.

Results

6-MDS inhibits proliferation of A459 cells

To verify the anti-proliferative effect of 6-MDS on LUAD, CCK8 was used to determine the cell viability after treatment with 6-MDS for 24 h and 48 h, respectively. Gradually elevating the concentrations of 6-MDS from 2 to 64 $\mu\text{g}/\text{mL}$ resulted in a dose-dependent decrease in the survival rates of LUAD cells (Fig. 1A-B), indicating a pronounced inhibitory influence of 6-MDS on LUAD cell proliferation. Specifically, 6-MDS inhibited the growth of A549 cells with an IC_{50} of $5.22 \pm 0.60 \mu\text{M}$ for 24 h and $2.90 \pm 0.38 \mu\text{M}$ for 48 h.

Prediction of LUAD and 6-MDS targets

Using the TCGA-LUAD cohort in GEPIA database, a total of 4,246 DEGs were identified and visually displayed through box plots, including 1,112 up-regulated and 3,134 down-regulated (Fig. 2A, Table S1). Besides, 9,642 LUAD targets were extracted from the above-mentioned three database: Drugbank, GeneCards and OMIM (Table

S2). Finally, 522 LUAD-related targets were obtained by Venn analysis (Table S3). As for the 6-MDS targets, a grand total of 379 target genes were secured from the PharmMapper, SuperPred, SwissTargetPrediction and targetnet (Table S4).

Targets of 6-MDS in LUAD acquisition and functional enrichment analysis

33 potential targets of 6-MDS in LUAD were identified by crossing the LUAD-related targets with 6-MDS targets (Fig. 2B, Table S5), which were then submitted to the Metascape database to explore the potential biological functions of these genes. The results of KEGG enrichment analysis indicated that these genes were significantly enriched in cell cycle, pyrimidine metabolism as well as transcriptional mis-regulation in cancer (Fig. 2C). Regarding GO analysis, the results demonstrated that these 33 potential targets of 6-MDS in LUAD were notably related to cell cycle G2/M phase transition, response to wounding and response to amyloid-beta (Fig. 2D). These outcomes imply that 6-MDS may mainly inhibit the occurrence of LUAD by affecting the cell cycle.

PPI network construction

The 33 potential targets of 6-MDS in LUAD were submitted to the STRING database to obtain the PPI data. The PPI data was then visualized and analyzed using Cytoscape software (Fig. 3A). Subsequently, the cytohubba plug-in was employed to analyze the PPI network and identify the top ten hub genes, which were then displayed in Table 1; Fig. 3B. Nodes in a darker shade of red indicate higher importance. The top 10 hub genes comprised MMP9, CDK1, TYMS, CCNA2, ERBB2, CHEK1, KIF11, AURKB, PLK1 and TTK. Further analysis through KEGG enrichment analysis indicated that these hub genes were primarily involved in the cell cycle and pathways in cancer signaling pathway (Fig. 3C).

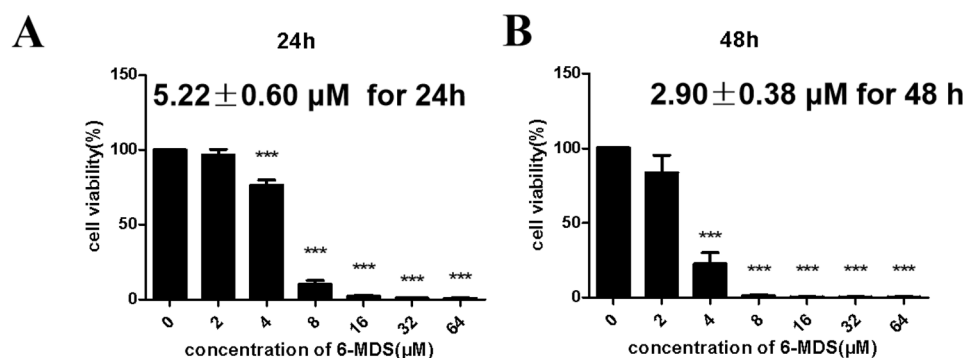


Fig. 1 Effect of 6-MDS on the viability of A549 for 24 h (A) and 48 h (B), respectively

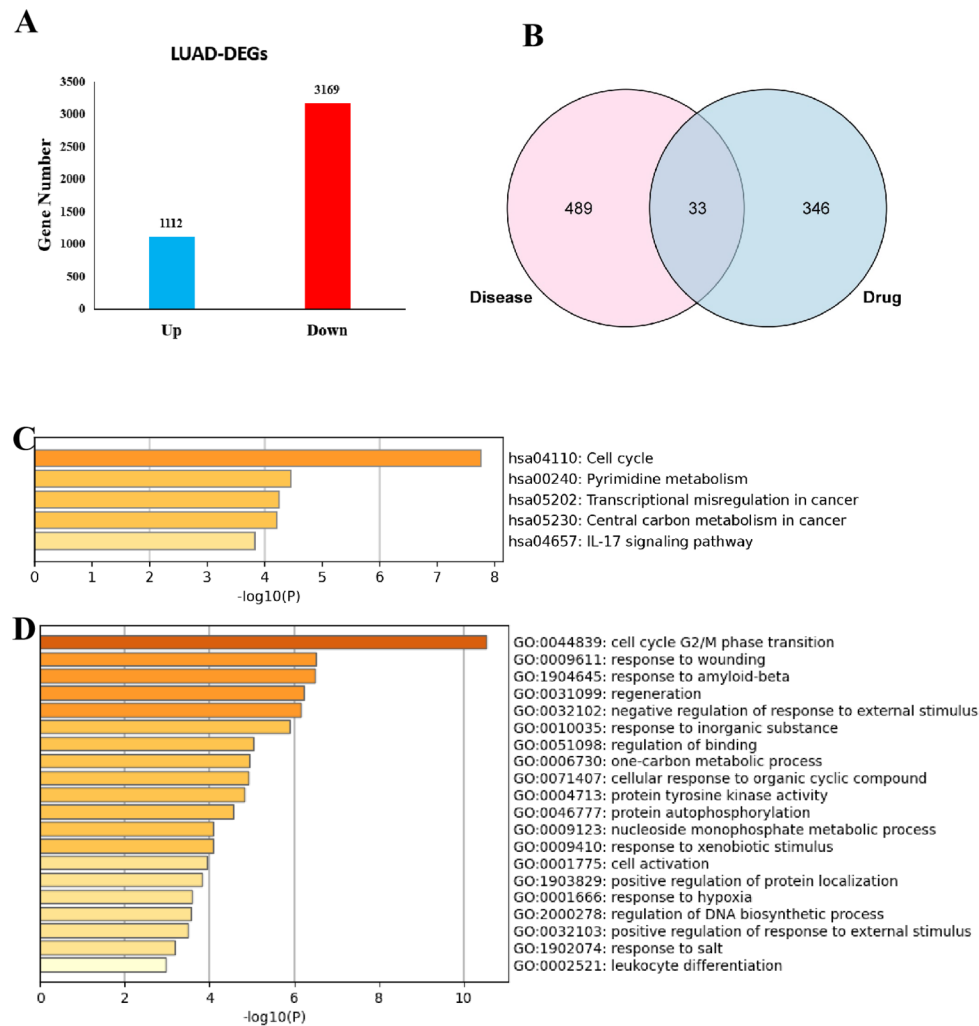


Fig. 2 Identification of the DEGs of LUAD in the TCGA cohort and Functional enrichment analysis. **A** Box plots to visualize the DEGs; **B** Venn diagram to identify 6-MDS-related targets for LUAD. **C** KEGG enrichment analysis of the 6-MDS-related targets for LUAD; **D** GO enrichment analysis of the 6-MDS-related targets for LUAD

Molecular docking validation of 6-MDS and 10 hub genes

In order to confirm the possibility of these 10 core genes as key targets for 6-MDS treatment of LUAD, AutoDockTools-1.5.6 software was used to perform virtual molecular docking between 6-MDS and these 10 hub genes. The PDB file of the target protein is downloaded and the details of the protein are collected from the PDB database (Table 2). The parameters of the docking box are collected (Table 3). The resulting binding energy, amino acid residues, hydrogen bonds and Kd value were shown in Table 4, the outcomes of molecular docking were visualized in Fig. 4. Notably, the binding energies between 6-MDS and the hub proteins were all higher than -6 kcal/mol except for AURKB, suggesting robust affinity between 6-MDS and 9 of the targets. Remarkably, the binding energy of 6-MDS with PLK1 was -11.90 kcal/mol, exhibiting the lowest docking energy among the 10 hub genes. In summary, the results indicated that 6-MDS

binds strongly to core target proteins, and 6-MDS may exert anti-cancer effects by binding to core target proteins.

External validation of the 9 hub genes

The mRNA expression levels of 9 hub genes

Since the AURKB showed no Binding energy with 6-MDS, it was excluded for further validation. The results from the GEPIA showed the expression level of the other 9 hub genes was much higher in cancer tissues than in normal tissues for LUAD (Fig. 5). Besides, the expression level of CDK1, CCNA2, CHEK1, KIF11, PLK1 and TTK was significantly elevated with cancer progression in LUAD (Fig. 6).

The protein expression levels of 9 hub genes

Consistent with the gene expression pattern, the protein expression levels of CDK1, TYMS, CCNA2,

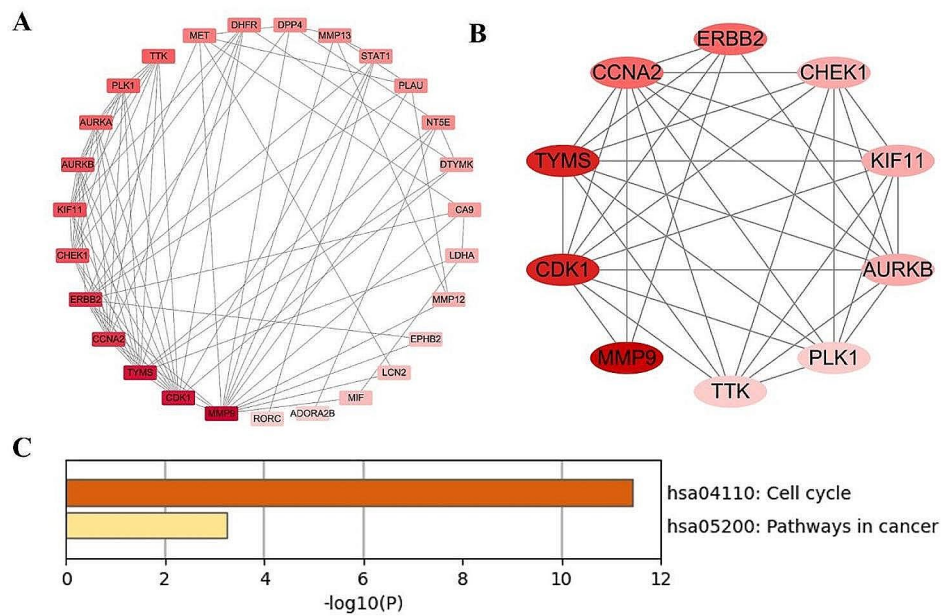


Fig. 3 PPI network and KEGG analyses of the ten core genes. **A** PPI network visualized by Cytoscape; **B** Network of interactions of top ten hub genes; **C** KEGG enrichment analysis of the top ten hub genes

Table 1 10 Hub genes identified using 4 different algorithms in the Cytohubba plug-in

Rank	Gene symbol	Full name	Degree
1	MMP9	Matrix metalloproteinase-9	14.00
2	CDK1	Cyclin-dependent kinase 1	13.00
3	TYMS	Thymidylate synthase	13.00
4	ERBB2	Receptor tyrosine-protein kinase erbB-2	11.00
5	CCNA2	Cyclin-A2	11.00
6	KIF11	Kinesin-like protein KIF11	9.00
7	AURKB	Aurora kinase B	9.00
8	CHEK1	Serine/threonine-protein kinase Chk1	9.00
9	PLK1	Serine/threonine-protein kinase PLK1	8.00
10	TTK	Dual specificity protein kinase TTK	8.00

Table 2 Details of the protein targets in the PDB database

Targets	PDB ID	Method	Resolution (Å)	R-Value free	R-Value work	R-Value observed
MMP9	1ITV	X-RAY DIFFRACTION	1.95 Å	0.275	0.229	0.232
CDK1	4YC6	X-RAY DIFFRACTION	2.60 Å	0.267	0.225	0.227
TYMS	1HZW	X-RAY DIFFRACTION	2.00 Å	0.239	0.206	\
CCNA2	1E9H	X-RAY DIFFRACTION	2.50 Å	0.273	0.225	0.225
ERBB2	1MFG	X-RAY DIFFRACTION	1.25 Å	0.165	0.128	0.130
KIF11	2G1Q	X-RAY DIFFRACTION	2.51 Å	0.279	0.234	0.234
PLK1	8BJT	X-RAY DIFFRACTION	2.19 Å	0.255	0.200	0.203
TTK	3CEK	X-RAY DIFFRACTION	2.30 Å	0.250	0.184	0.188
CHEK1	6FCK	X-RAY DIFFRACTION	1.90 Å	0.214	0.174	0.176
AURKB	4AF3	X-RAY DIFFRACTION	2.75 Å	0.264	0.205	0.208

Table 3 Grid docking parameters in molecular docking

Target name	PDB ID	Spacing (angstrom)	X center	Y Center	Z center
MMP9	1ITV	1.000	-27.273	-40.514	-12.717
CDK1	4YC6	1.000	-14.325	12.348	-22.280
TYMS	1HZW	1.000	8.628	75.574	10.988
CCNA2	1E9H	0.981	11.114	27.215	90.265
ERBB2	1MFG	0.375	8.805	5.734	26.156
KIF11	2G1Q	0.964	29.537	5.655	79.451
PLK1	8BJT	0.886	-26.980	22.791	-9.754
TTK	3CEK	0.786	-4.222	16.249	34.182
CHEK1	6FCK	0.847	14.054	0.245	35.894
AURKB	4AF3	0.983	15.553	-16.602	-3.528

Table 4 Basic information on the molecular docking of 6-MDS and target proteins

Mo-lecu-lar name	Targets	PDB ID	Residue involved in H bonding	Binding energy (kcal/Mol)	Kd(mol/L)
6-MDS	MMP9	1ITV	ALA-159	-8.30	8.12×10^{-7}
6-MDS	CDK1	4YC6	ARG-20,LEU-46	-8.70	4.13×10^{-7}
6-MDS	TYMS	1HZW	CYS-195	-9.40	1.27×10^{-7}
6-MDS	CCNA2	1E9H	TRP-227	-8.00	1.35×10^{-6}
6-MDS	ERBB2	1MFG	SER-1278,ARG-1307	-6.90	8.64×10^{-6}
6-MDS	KIF11	2G1Q	LYS-315	-8.00	1.35×10^{-6}
6-MDS	PLK1	8BJT	ASP-194	-11.90	1.85×10^{-9}
6-MDS	TTK	3CEK	LYS-553	-8.70	4.13×10^{-7}
6-MDS	CHEK1	6FCK	LYS-38	-9.40	1.27×10^{-7}
6-MDS	AURKB	4AF3	/	/	/

ERBB2, CHEK1, KIF11 and PLK1 in LUAD tissues was

significantly up-regulated compared with normal lung tissues (Fig. 7). However, the protein expression level of MMP9 was significantly down-regulated in LUAD tissue compared with normal lung tissues, which was contrary to its gene expression pattern and needs to be verified through subsequent experiments.

Overall survival analysis of 9 hub genes

As for overall survival analysis of 9 hub genes, the results indicated that high expression of eight out of ten hub genes, including CDK1, TYMS, CCNA2, CHEK1, KIF11, PLK1 and TTK were significantly associated with the OS of LUAD patients (Fig. 8).

Analysis of promotor methylation level of hub genes

The dysregulation of DNA methylation has been implicated in the development of cancer, and used for cancer diagnosis and therapy [47, 48]. Therefore, the DNA methylation level of the 9 hub genes were compared between normal and cancer tissues by using the UALCAN databases. The result revealed that the promotor methylation level of TYMS, ERBB2, CHEK1, KIF11, PLK1 and TTK were significantly decreased in LUAD tissues compared with that in normal tissues (Fig. 9).

Immune cell infiltration of hub genes

The 9 hub genes effects on the immunological milieu of tumors were investigated by assessing the association of its expression with the degree of immune cell infiltration. As is shown in Fig. 10, the expression of CCNA2, CDK1 and TTK were positively correlated with the infiltration of CD8+T cells and neutrophils, while it was negatively

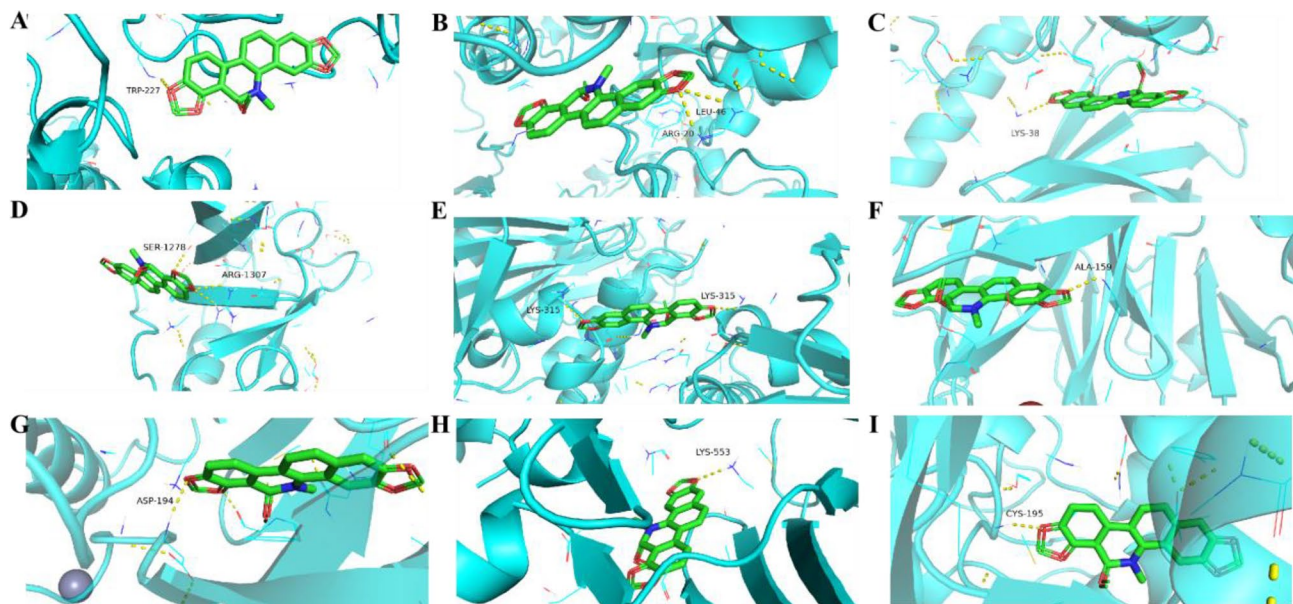


Fig. 4 Molecular docking pattern of 6-MDS and core target protein. **A** 6-MDS-CCNA2; **B** 6-MDS-CDK1; **C** 6-MDS-CHEK1; **D** 6-MDS-ERBB2; **E** 6-MDS-KIF11; **F** 6-MDS-MMP9; **G** 6-MDS-PLK1; **H** 6-MDS-TTK; **I** 6-MDS-TYMS

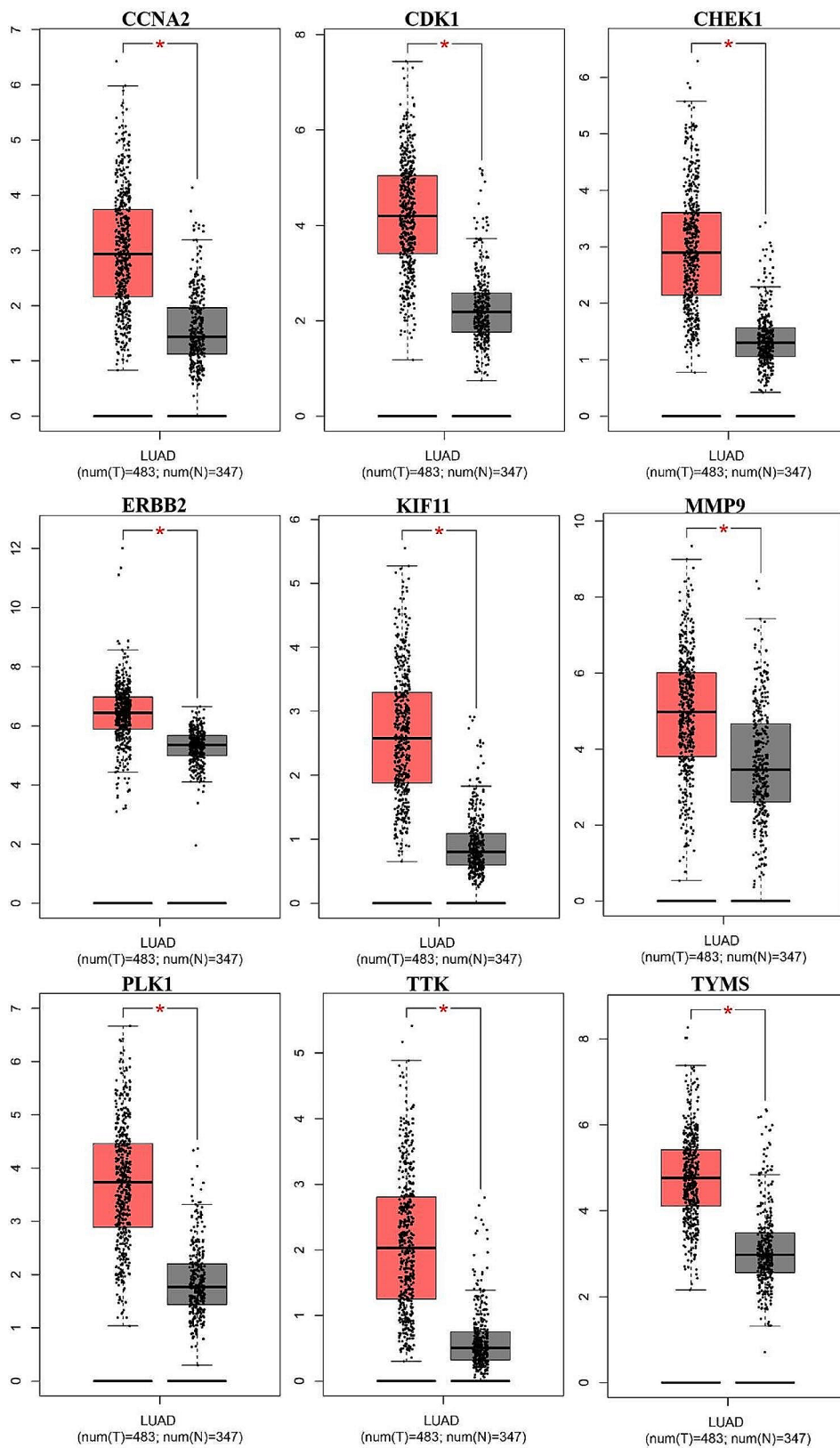


Fig. 5 Box plot of hub gene mRNA expression levels in the GEPIA database. Red represents tumor tissues and gray represents normal tissues

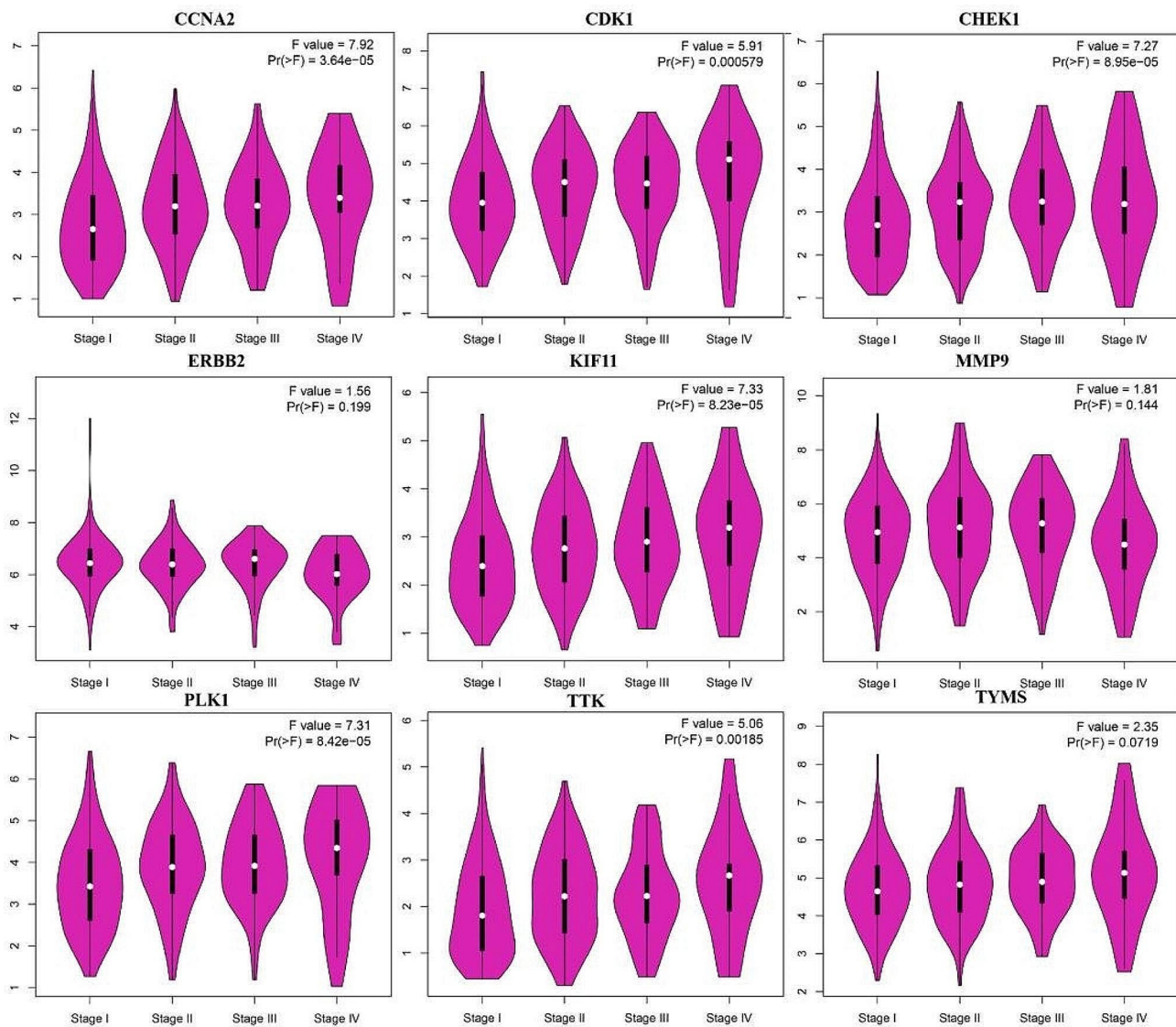


Fig. 6 Stage diagram of hub gene mRNA expression levels and pathological stages in the GEPIA database

correlated with the infiltration of B cell and CD4+ T cell. The expression of CHEK1 and KIF11 were positively correlated with infiltration of neutrophils, while negatively correlated with B cells. As for ERBB2, its expression level was negatively correlated with the infiltration of CD8+ T cell and positively correlated with the infiltration of B cell. The expression of PLK1 and TYMS were positively correlated with infiltration of neutrophils cells, while negatively correlated with the infiltration of B cell. The expression level of MMP9 was negatively correlated with purity, while positively related to the infiltration of B cell, CD4+ T cell, Macrophage, neutrophil and Dendritic cell.

Correlation of hub genes expression with immune subtypes

The TISIDB online tool was utilized to analyze the relationship between the 9 hub genes expression and LUAD

immune subtypes. The results obtained from the TISIDB indicated that the expression level of the 9 hub genes was significantly associated with different immune subtypes in LUAD (Fig. 11).

6-MDS down-regulated the mRNA expression level of target genes

Since CDK1, CHEK1, KIF11, PLK1 and TTK was significantly elevated with cancer progression in LUAD and exhibited excellent binding performance with 6-MDS, they were chosen for further validation. The results of qPCR indicated that after the intervention of 5 μ M 6-MDS for 24 h, the mRNA expression of CDK1, CHEK1, KIF11, PLK1 and TTK decreased significantly compared with the untreated group ($P < 0.05$). (Fig. 12A-E).

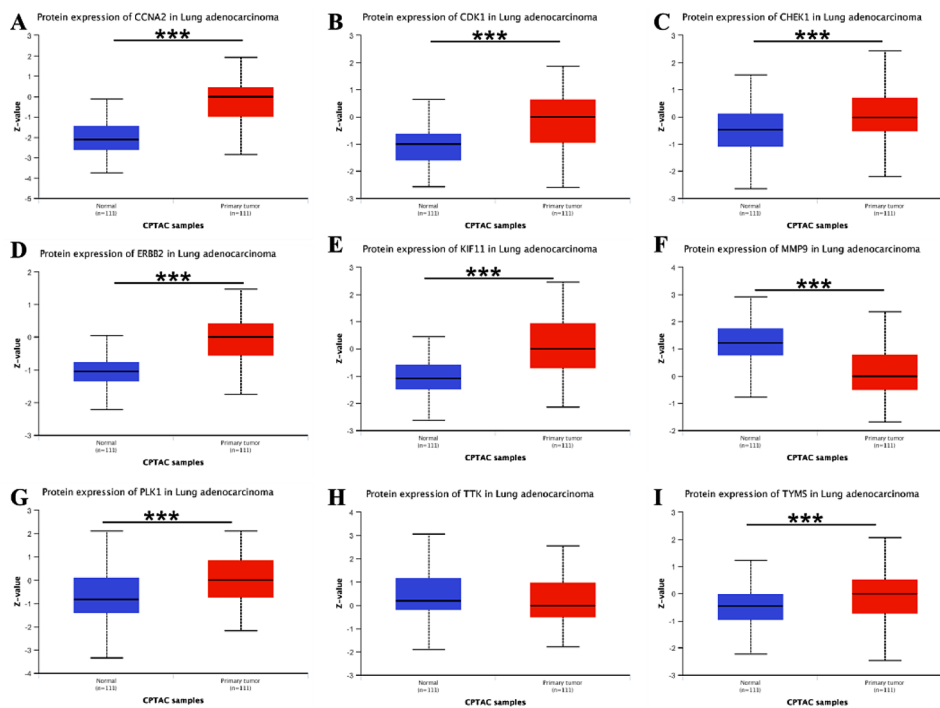


Fig. 7 Box plot of hub protein expression levels in the UALCAN database. Red represents tumor tissues and Blue represents normal tissues. **A** CCNA2; **B** CDK1; **C** CHEK1; **D** ERBB2; **E** KIF11; **F** MMP9; **G** PLK1; **H** TTK; **I** TYMS

Discussion

Lung cancer is the leading cause of mortality from cancer worldwide. Lung adenocarcinoma (LUAD) is a type of non-small cell lung cancer (NSCLC) with highest prevalence. Despite advancements in targeted therapy and immunotherapy, the overall survival of LUAD patients remain discouraging due to the metastases [49]. Natural products have recently garnered significant interest owing to their potential anti-cancer effects, which could pave the way for the development of innovative medications. 6-MDS is a natural benzophenanthridine alkaloid [50] which has shown promising anti-cancer effects. However, whether 6-MDS exhibits anti-cancer properties on LUAD and the underlying pharmacological mechanism needs further study.

In recent decades, the integration of network-based pharmacology and computer-assisted drug design technology has gained traction in uncovering the intricate workings of drugs, emerging as a potent approach in pharmaceutical investigations [51–55]. Among them, network pharmacology enables the anticipation of disease targets impacted by drugs, while molecular docking facilitates the examination of drug-gene interactions. In this study, a combination of bio-information analysis and network pharmacology, as well as molecular docking, were used to simulate the possible mechanisms of 6-MDS treatment for LUAD. Through network pharmacology, we identified 10 core genes that may be potential targets

for 6-MDS treatment of LUAD. KEGG enrichment analysis revealed that these genes were mainly enriched in cell cycle pathway. Cell cycle regulation is orchestrated by a complex network of interactions between proteins, enzymes, cytokines, and cell cycle signaling pathways, and is vital for cell proliferation, growth, and repair. It is well-established that the occurrence, development, and metastasis of tumors are intricately linked with the regulation of the cell cycle [56]. These finding proposed that 6-MDS may mainly inhibit the occurrence of LUAD by affecting the cell cycle.

The molecular docking analysis unveiled that nine targets had good binding performance with 6-MDS. Notably, the binding energy of 6-MDS with PLK1 was -11.90 kcal/mol, which had the lowest docking energy among the targets examined. Besides, the binding energy of CDK1, CHEK1, KIF11 and TTK were all lower than -8.7 kcal/mol, indicating strong binding capabilities. In addition, the expression level of CDK1, CHEK1, KIF11, PLK1 and TTK was significantly elevated with cancer progression in LUAD. And they also demonstrated a significant correlation with the OS of LUAD patients.

Polo-like kinase 1 (PLK1) is crucial for the normal progression of mitosis. The significant upregulation of PLK1 has been found in various human cancers and is significantly associated with poor prognosis in various cancers. Many studies have showed that inhibition of PLK1 could lead to death of cancer cells by interfering with multiple

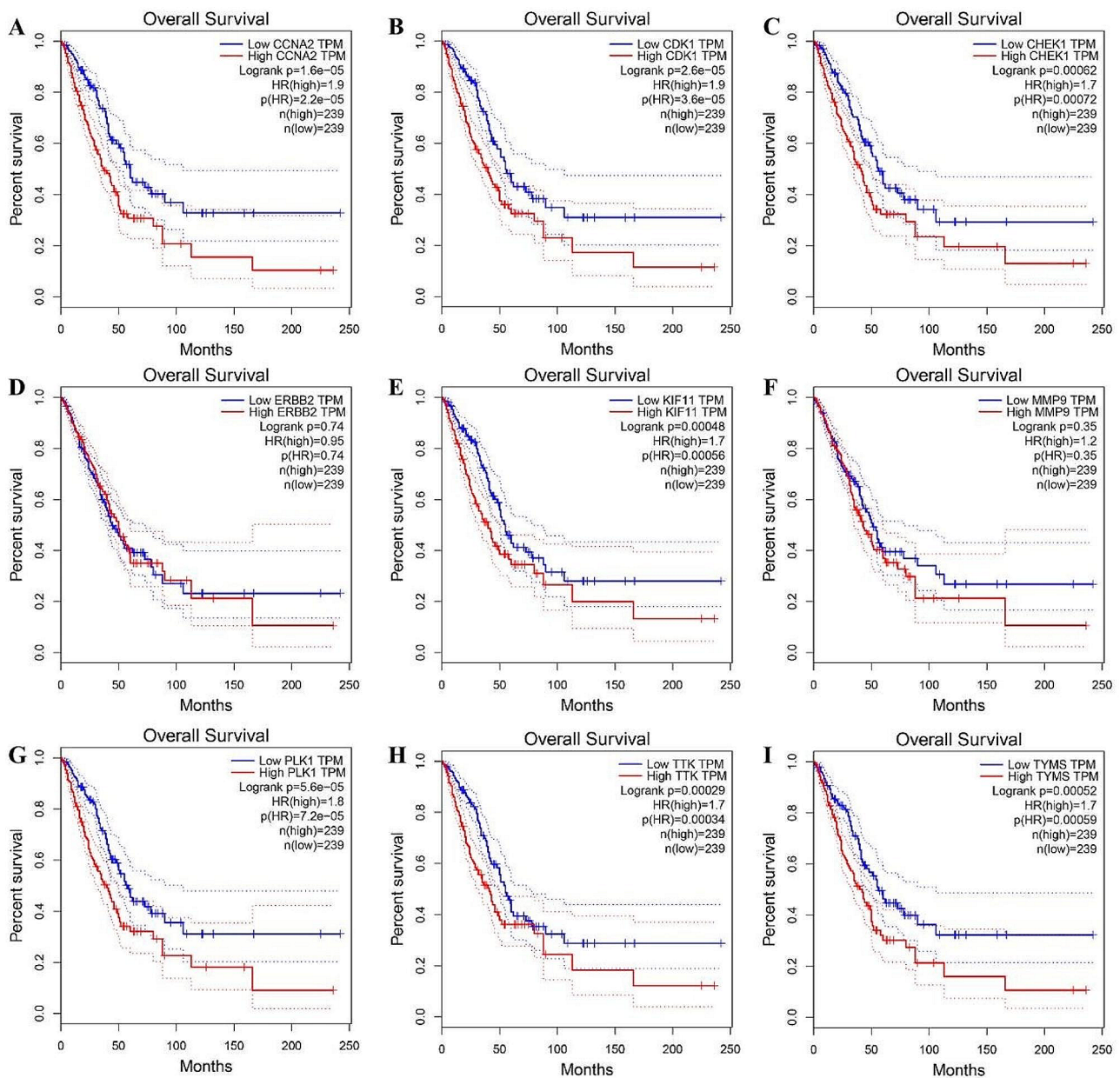


Fig. 8 Overall survival analysis of hub gene in the GEPIA database. **A** CCNA2; **B** CDK1; **C** CHEK1; **D** ERBB2; **E** KIF11; **F** MMP9; **G** PLK1; **H** TTK; **I** TYMS

stages of mitosis. In the case of LUAD, PLK1 was found to be highly expressed in LUAD and was positively associated with advanced disease staging and poor survival outcomes. Also, PLK1 plays a critical role in LUAD progression by regulating necroptosis and immune infiltration, and may serve as a potential therapeutic target for immunotherapy [57, 58]. Cyclin dependent kinases (CDKs) are serine/threonine kinases that are proposed as promising candidate targets for cancer treatment [59]. Deregulation of CDK1 has been shown to be closely associated with tumorigenesis. CDK1 activation plays a critical role in a wide range of cancer types; and CDK1 phosphorylation of its many substrates greatly influences

their function in tumorigenesis. These proteins complexed with cyclins play a critical role in cell cycle progression. CDK1 is a potential prognostic biomarker and target for lung cancer; CDK1 activity is critical for JAK/STAT3 signaling activation, and the inhibition of CDK1 can suppress lung cancer. In addition, an in vitro study of LUAD cells showed that reduced CDK1 activity led to cell cycle arrest and promotion of apoptosis in LUAD [60]. Hence, CDK1 may be used as potential biomarkers and therapeutic targets for LUAD [61]. Checkpoint kinase 1 (CHEK1, also known as CHK1) is a conserved serine/threonine kinase that plays an important role in replication fork stability and DNA damage response [62]. In a

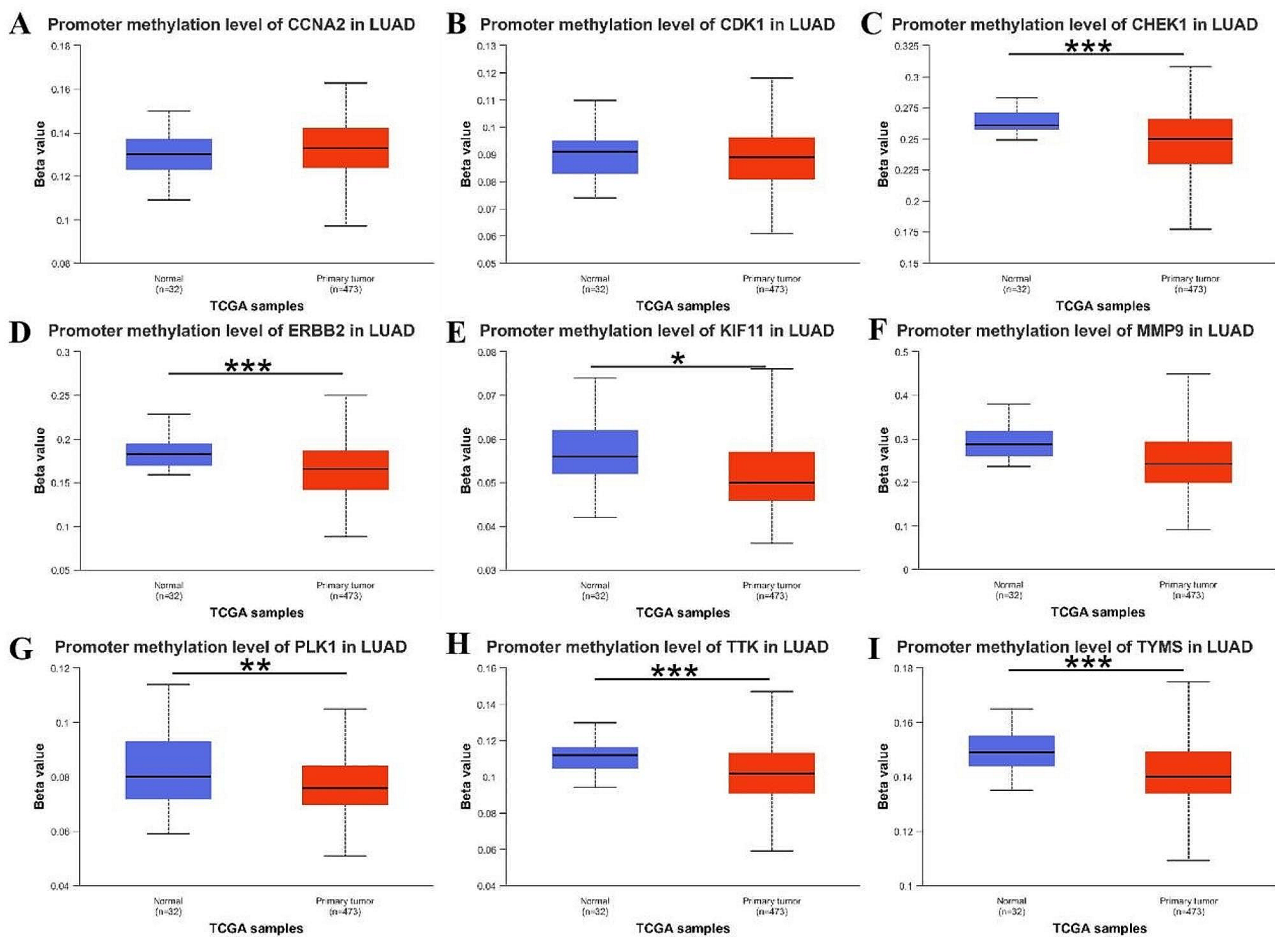


Fig. 9 Promoter methylation level of hub genes in the UALCAN database. **A** CCNA2; **B** CDK1; **C** CHEK1; **D** ERBB2; **E** KIF11; **F** MMP9; **G** PLK1; **H** TTK; **I** TYMS

study of TP53 mutant NSCLC tumor cells, it was found that inhibiting the expression of CHEK1 can significantly enhance the sensitivity of tumor cells to chemotherapy [63, 64]. In addition, promoter methylation, amplification, and miRNA regulation in patients with lung adenocarcinoma may lead to the upregulation of the CHEK1 gene, which may be a marker for predicting the survival rate of patients with lung adenocarcinoma [65]. The motor protein superfamily consists of 45 family members, among which KIF11 plays a role as a motor protein in mitosis. KIF11 is essential for LUAD cell proliferation and metastasis, and it may serve as an independent prognostic factor as well as a promising therapeutic target for LUAD patients [66]. TTK, also known as Monopolar spindle1 (Mps1), is the crucial modulator of the spindle assembly checkpoint, which is responsible for ensuring chromosomal separation. At present, some studies have found that TTK may be related to the occurrence and development of lung cancer. Zheng et al. showed that the expression of TTK was higher in lung adenocarcinoma and squamous cell carcinoma than in normal lung tissue, which was related to the poor prognosis of patients with

lung adenocarcinoma [67]. When TTK was knocked out in A549 cell, cell proliferation, migration and tumorigenesis were inhibited [68]. Therefore, TTK may be a promising prognostic biomarker for LUAD and is worthy of further investigation [69]. Furthermore, qPCR resulted indicated that after the intervention of 5 μ M 6-MDS for 24 h, the mRNA expression of CDK1, CHEK1, KIF11, PLK1 and TTK decreased significantly compared with the untreated group. In conclusion, the 5 key targets, which had good binding force with 6-MDS may play an important role in cancer progression, which preliminarily confirmed the possibility of 6-MDS against LUAD at the molecular level.

Our present study has certain limitations. Firstly, this study reveals possible targets and pathways of the impact of 6-MDS, but our understanding of the exact mechanism by which 6-MDS exerts its anti-tumor properties is still quite limited. Deeper exploration into the downstream signaling pathways and molecular mechanisms that drive the activity of 6-MDS could provide valuable insights into the discovery. Secondly, it is not hard to argue that more accurate experiments should be carried

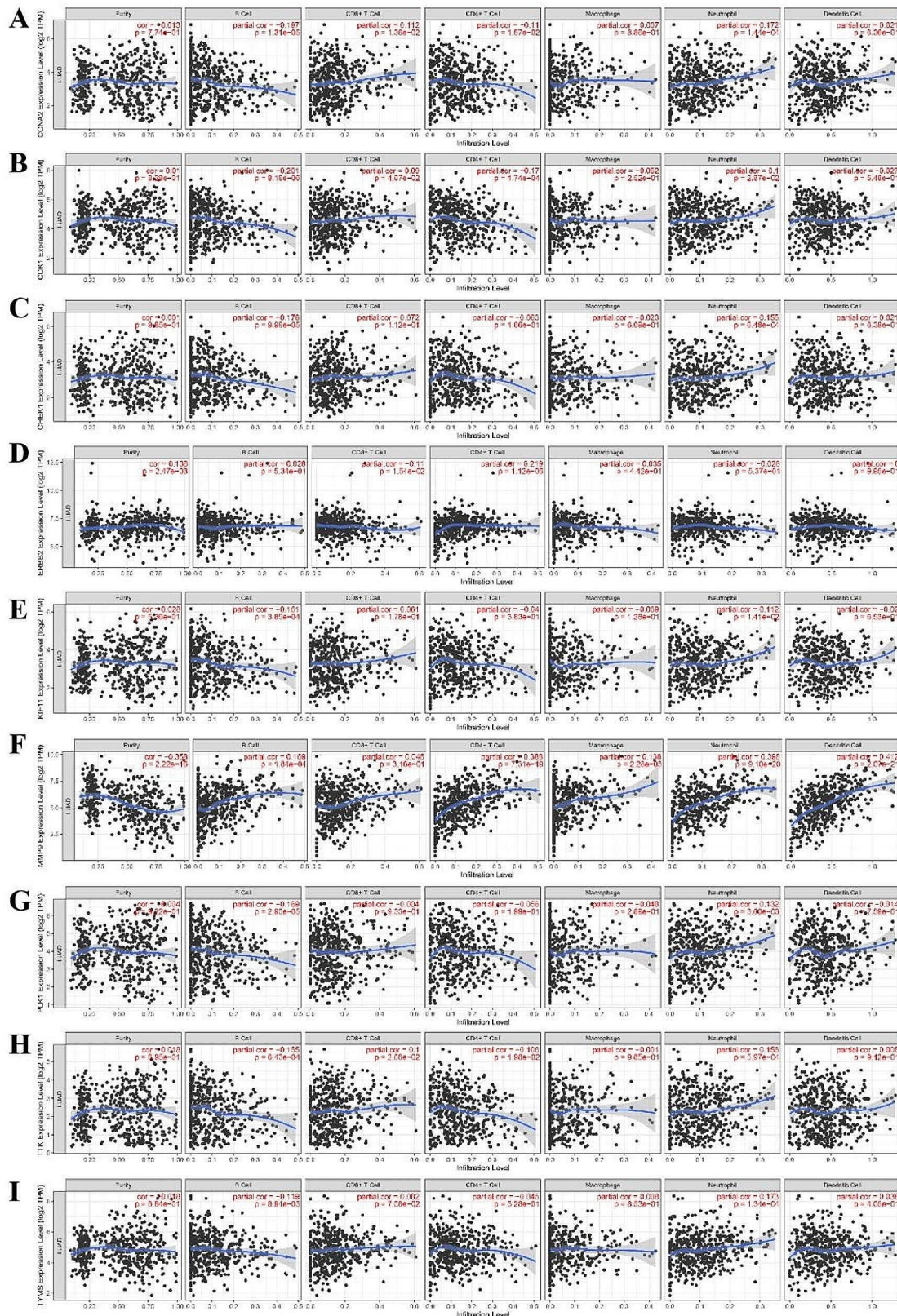


Fig. 10 Immune cell infiltration of core targets in the Tisler database. **A** CCNA2; **B** CDK1; **C** CHEK1; **D** ERBB2; **E** KIF11; **F** MMP9; **G** PLK1; **H** HTK; **I** ITYMS

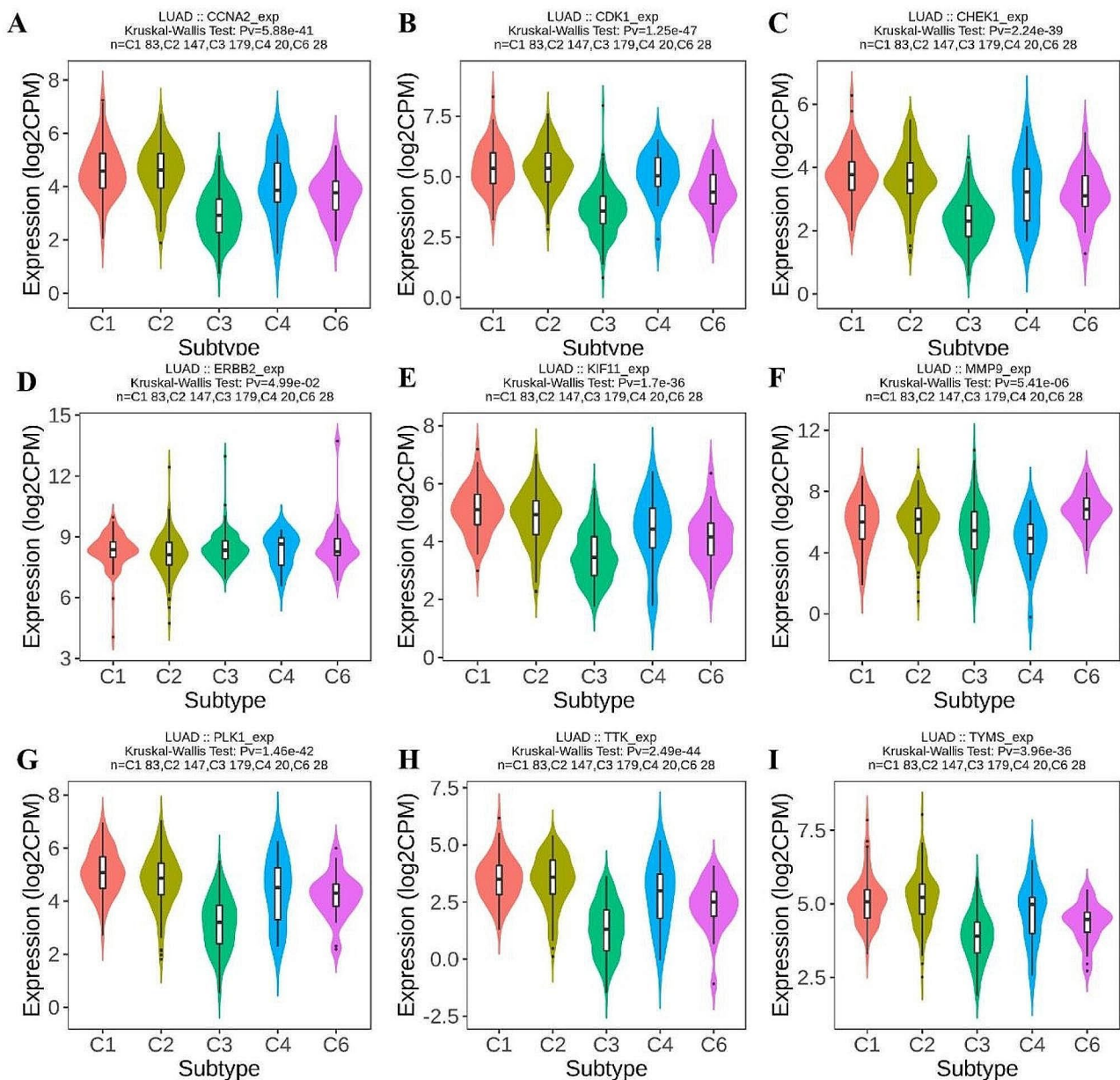


Fig. 11 Correlation of hub genes expression with immune subtypes in the TISIDB database. **A** CCNA2; **B** CDK1; **C** CHEK1; **D** ERBB2; **E** KIF11; **F** MMP9; **G** PLK1; **H** TTK; **I** TYMS

out, such as surface plasmon resonance (SPR) or Cellular Thermal Shift Assay (CETSA) to confirm that 6-MDS does indeed treat lung adenocarcinoma through the above mentioned targets. Furthermore, the incorporation of animal models or clinical trials is imperative to establish stronger evidence regarding the efficacy and safety of 6-MDS for LUAD treatment. Nevertheless, the current limitations in resources and time have confined us to performing only fundamental experiments. Thirdly, it should be noted that the limited water solubility and fast metabolism of 6-MDS may hinder its medical applications, despite its encouraging anti-cancer properties.

Therefore, innovative approaches like nanocarriers need to be developed and explored to enhance the bioavailability of 6-MDS. The next phase of our research will focus on this particular area.

Conclusions

To sum up, a comprehensive evaluation of 6-MDS was performed for revealing its potential mechanism for the treatment of LUAD through network pharmacology, molecular docking and experimental validation. The results of this study suggested that 6-MDS might be a candidate used for treating LUAD. More studies are

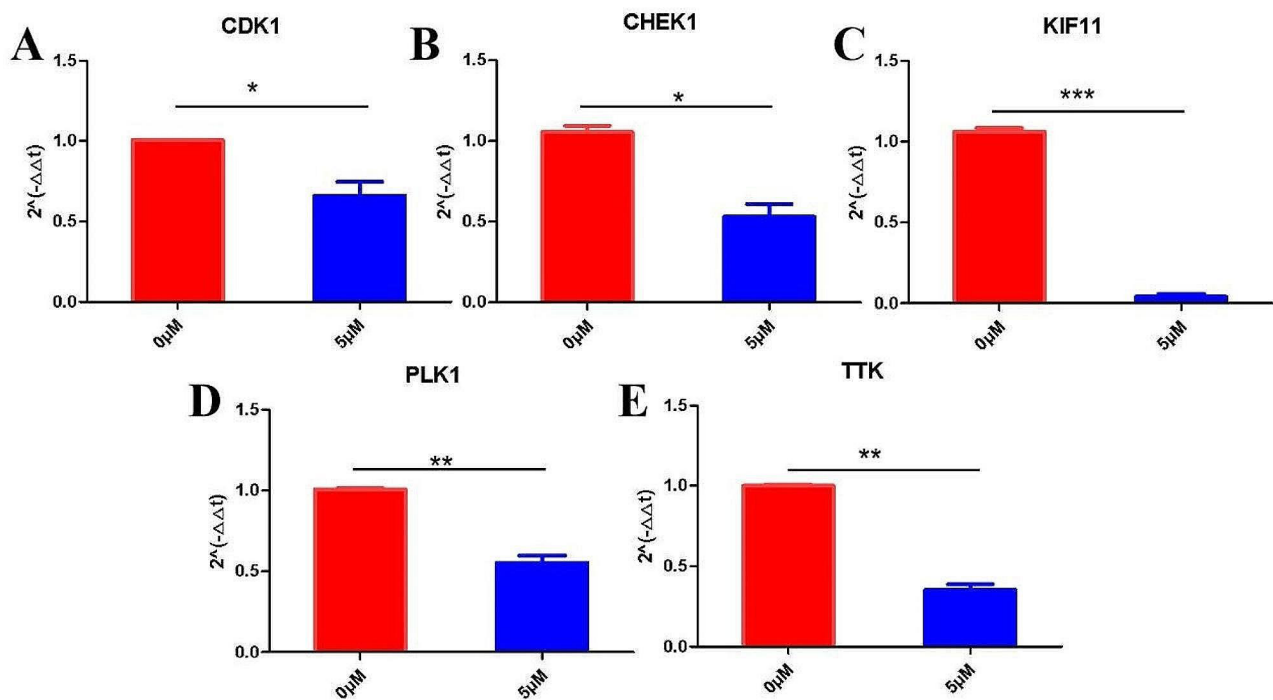


Fig. 12 Effect of 6-MDS on the expressions of CDK1, CHEK1, KIF11, PLK1, and TTK were detected using qRT-PCR assay (A-E)

required to validate its anti-cancer effect and explore the underlying mechanisms.

Supplementary Information

The online version contains supplementary material available at <https://doi.org/10.1186/s12906-024-04497-z>.

Supplementary Material 1

Acknowledgements

Not applicable.

Author contributions

XY L analyzed the data, prepared the figures and tables and wrote the manuscript. YL R participated in analyzing the data. ZR Y and SL Q reviewed, edited and revised the manuscript. All authors contributed to the article and approved the submitted version.

Funding

This work was supported by grants from the Hunan Provincial Natural Science Foundation of China (No.2022JJ40405), the National Natural Science Foundation of China (No.82204657 and No.82204250), China Postdoctoral Science Foundation (No. 2021M693961), National Key Clinical Specialty Construction Project (Clinical Pharmacy) and High Level Clinical Key Specialty (Clinical Pharmacy) in Guangdong Province.

Data availability

The original contributions presented in the study are included in the article/supplementary material. All other relevant data are available from the corresponding authors upon reasonable request.

Declarations

Ethics approval and consent to participate

Not applicable.

Consent for publication

Not applicable.

Competing interests

The authors declare no competing interests.

Author details

¹The Affiliated Nanhua Hospital, Hengyang Medical School, University of South China, Hengyang 421000, China

²Key Specialty of Clinical Pharmacy, The First Affiliated Hospital of Guangdong Pharmaceutical University, Guangzhou 510000, China

³School of Pharmacy, Xianning Medical College, Hubei University of Science and Technology, Xianning 437000, China

⁴NMPA Key Laboratory for Technology Research and Evaluation of Pharmacovigilance, Guangdong Pharmaceutical University, Guangzhou 510086, China

Received: 26 January 2024 / Accepted: 10 May 2024

Published online: 23 May 2024

References

- Zhang K, Qian Y, Quan X, et al. A Novel signature of lipid metabolism-related gene predicts prognosis and response to Immunotherapy in Lung Adenocarcinoma[J]. *Front Cell Dev Biol.* 2022;10:730132.
- Bray F, Laversanne M, Sung H. Global cancer statistics 2022: GLOBOCAN estimates of incidence and mortality worldwide for 36 cancers in 185 countries[J]. 2024.
- Sharma R. Mapping of global, regional and national incidence, mortality and mortality-to-incidence ratio of lung cancer in 2020 and 2050[J]. *Int J Clin Oncol.* 2022;27(4):665–75.

4. Pascoe HM, Knipe HC, Pascoe D, et al. The many faces of lung adenocarcinoma: a pictorial essay[J]. *J Med Imaging Radiat Oncol*. 2018;62(5):654–61.
5. Sung H, Ferlay J, Siegel RL, et al. Global Cancer statistics 2020: GLOBOCAN estimates of incidence and Mortality Worldwide for 36 cancers in 185 Countries[J]. *CA Cancer J Clin*. 2021;71(3):209–49.
6. Nawaz K, Webster RM. The non-small-cell lung cancer drug market[J]. *Nat Rev Drug Discov*. 2023;22(4):264–5.
7. Zeng Y, Pan Y, Zhang B, et al. Integrating Network Pharmacology, Molecular Docking, and experimental validation to investigate the mechanism of (-)-Guaio against Lung Adenocarcinoma[J]. *Med Sci Monit*. 2022;28:e937131.
8. Liu K, Fu X, Wang Z, et al. Integrating network pharmacology prediction and experimental investigation to verify ginkgetin anti-invasion and metastasis of human lung adenocarcinoma cells via the Akt/GSK-3 β /Snail and Wnt/ β -catenin pathway[J]. *Front Pharmacol*. 2023;14:1135601.
9. Kryczka J, Kryczka J. Molecular mechanisms of Chemoresistance Induced by Cisplatin in NSCLC Cancer Therapy[J]. 2021, 22(16).
10. Liu S, Yang P, Wang L et al. Targeting PAK4 reverses cisplatin resistance in NSCLC by modulating ER stress[J]. 2024, 10(1): 36.
11. Du R, Wang X, Ma L, et al. Adverse reactions of targeted therapy in cancer patients: a retrospective study of hospital medical data in. China[J]. 2021;21(1):206.
12. Kennedy LB, Salama. A K S. A review of cancer immunotherapy toxicity[J]. *CA Cancer J Clin*. 2020;70(2):86–104.
13. He Y, Zhao Y, Akhtar ML, et al. Neoadjuvant therapy for non-small cell lung cancer and esophageal cancer[J]. *Am J Cancer Res*. 2024;14(3):1258–77.
14. Li H, Zhou L, Zhou J, et al. Underlying mechanisms and drug intervention strategies for the tumour microenvironment[J]. *J Exp Clin Cancer Res*. 2021;40(1):97.
15. Wang S, Fu JL, Hao HF, et al. Metabolic reprogramming by traditional Chinese medicine and its role in effective cancer therapy[J]. *Pharmacol Res*. 2021;170:105728.
16. Liu TJ, Hu S, Qiu ZD, et al. Anti-tumor mechanisms Associated with Regulation of non-coding RNA by active ingredients of Chinese Medicine: a Review[J]. *Front Oncol*. 2020;10:634936.
17. He Q, Liu C, Wang X, et al. Exploring the mechanism of curcumin in the treatment of colon cancer based on network pharmacology and molecular docking[J]. *Front Pharmacol*. 2023;14:1102581.
18. Liu X, Liu Y, Huang P, et al. The Genome of Medicinal Plant *Macleaya cordata* provides New insights into Benzylisoquinoline Alkaloids Metabolism[J]. *Mol Plant*. 2017;10(7):975–89.
19. Liu ZH, Wang WM, Zhang Z, et al. Natural antibacterial and antivirulence alkaloids from *Macleaya cordata* against Methicillin-Resistant *Staphylococcus aureus*[J]. *Front Pharmacol*. 2022;13:813172.
20. Zhang L, Zhang X, Che D, et al. 6-Methoxydihydroanguinarine induces apoptosis and autophagy in breast cancer MCF-7 cells by accumulating ROS to suppress the PI3K/AKT/mTOR signaling pathway[J]. *Phytother Res*. 2023;37(1):124–39.
21. Lee YJ, Yin HQ, Kim YH, et al. Apoptosis inducing effects of 6-methoxydihydroanguinarine in HT29 colon carcinoma cells[J]. *Arch Pharm Res*. 2004;27(12):1253–7.
22. Yin HQ, Kim YH, Moon CK, et al. Reactive oxygen species-mediated induction of apoptosis by a plant alkaloid 6-methoxydihydroanguinarine in HepG2 cells[J]. *Biochem Pharmacol*. 2005;70(2):242–8.
23. Wang LL, Li RT, Zang ZH, et al. 6-Methoxydihydroanguinarine exhibits cytotoxicity and sensitizes TRAIL-induced apoptosis of hepatocellular carcinoma cells through ROS-mediated upregulation of DR5[J]. *Med Oncol*. 2023;40(9):266.
24. Luo TT, Lu Y, Yan SK, et al. Network Pharmacology in Research of Chinese Medicine Formula: methodology, application and Prospective[J]. *Chin J Integr Med*. 2020;26(1):72–80.
25. Ling J, Wang Y, Ma L et al. Exploration of Potential Targets and Mechanisms of Fisetin in the Treatment of Non-Small-Cell Lung Carcinoma via Network Pharmacology and In Vitro Validation[J]. *Evid Based Complement Alternat Med*. 2022, 2022: 2383527.
26. Deng T, Xie L, Xiaofang C et al. ATM-Mediated translocation of RanBPM regulates DNA damage response by stabilizing p21 in non-small cell lung cancer cells[J]. *Cell Oncol (Dordr)*, 2023.
27. Peng Y, Tang R, Ding L, et al. Diosgenin inhibits prostate cancer progression by inducing UHRF1 protein degradation[J]. *Eur J Pharmacol*. 2023;942:175522.
28. Kim S, Chen J. PubChem 2023 update[J]. 2023, 51(D1): D1373–80.
29. Wang X, Shen Y, Wang S, et al. PharmMapper 2017 update: a web server for potential drug target identification with a comprehensive target pharmacophore database[J]. *Nucleic Acids Res*. 2017;45(W1):W356–60.
30. Gallo K, Goede A. SuperPred 3.0: drug classification and target prediction-a machine learning approach[J]. 2022, 50(W1): W726–31.
31. Daina A, Michielin O, Zoete V. SwissTargetPrediction: updated data and new features for efficient prediction of protein targets of small molecules[J]. *Nucleic Acids Res*. 2019;47(W1):W357–64.
32. Yao ZJ, Dong J, Che YJ, et al. TargetNet: a web service for predicting potential drug-target interaction profiling via multi-target SAR models[J]. *J Comput Aided Mol Des*. 2016;30(5):413–24.
33. UniProt. The Universal protein knowledgebase in 2023[J]. *Nucleic Acids Res*. 2023;51(D1):D523–31.
34. Tang Z, Li C, Kang B, et al. GEPIA: a web server for cancer and normal gene expression profiling and interactive analyses[J]. *Nucleic Acids Res*. 2017;45(W1):W98–102.
35. Amberger JS, Bocchini CA, Scott AF, et al. OMIM.org: leveraging knowledge across phenotype-gene relationships[J]. *Nucleic Acids Res*. 2019;47(D1):D1038–43.
36. Knox C, Wilson M, Klinger CM et al. DrugBank 6.0: the DrugBank Knowledgebase for 2024[J]. 2024, 52(D1): D1265-d1275.
37. Stelzer G, Rosen N, Plaschkes I et al. The GeneCards suite: from Gene Data Mining to Disease Genome sequence Analyses[J]. *Curr Protocols Bioinf*, 2016, 54(1): 1.30.31–31.30.33.
38. Zhou Y, Zhou B, Pache L, et al. Metascape provides a biologist-oriented resource for the analysis of systems-level datasets[J]. *Nat Commun*. 2019;10(1):1523.
39. Szklarczyk D, Kirsch R, Koutrouli M. The STRING database in 2023: protein-protein association networks and functional enrichment analyses for any sequenced genome of interest[J]. 2023, 51(D1): D638–46.
40. Shannon P, Markiel A, Ozier O, et al. Cytoscape: a software environment for integrated models of biomolecular interaction networks[J]. *Genome Res*. 2003;13(11):2498–504.
41. Pinzi L, Rastelli G. Molecular Docking: shifting paradigms in Drug Discovery[J]. *Int J Mol Sci*, 2019, 20(18).
42. Xue LC, Rodrigues JP, Kastiris PL, et al. PRODIGY: a web server for predicting the binding affinity of protein-protein complexes[J]. *Bioinformatics*. 2016;32(23):3676–8.
43. Chandrashekar DS, Karthikeyan SK, Korla PK, et al. UALCAN: an update to the integrated cancer data analysis platform[J]. *Neoplasia*. 2022;25:18–27.
44. Chen F, Zhang Y, Chandrashekar DS, et al. Global impact of somatic structural variation on the cancer proteome[J]. *Nat Commun*. 2023;14(1):5637.
45. Li T, Fu J, Zeng Z, et al. TIMER2.0 for analysis of tumor-infiltrating immune cells[J]. *Nucleic Acids Res*. 2020;48(W1):W509–14.
46. Ru B, Wong CN, Tong Y, et al. TISIDB: an integrated repository portal for tumor-immune system interactions[J]. *Bioinformatics*. 2019;35(20):4200–2.
47. Klutstein M, Nejman D, Greenfield R, et al. DNA methylation in Cancer and Aging[J]. *Cancer Res*. 2016;76(12):3446–50.
48. Ibrahim J, Op de Beeck K, Fransens E, et al. Genome-wide DNA methylation profiling and identification of potential pan-cancer and tumor-specific biomarkers[J]. *Mol Oncol*. 2022;16(12):2432–47.
49. Shih DJH, Nayyar N, Bihun I, et al. Genomic characterization of human brain metastases identifies drivers of metastatic lung adenocarcinoma[J]. *Nat Genet*. 2020;52(4):371–7.
50. Peng R, Xu M, Xie B et al. Insights on Antitumor activity and mechanism of natural benzophenanthridine Alkaloids[J]. *Molecules*, 2023, 28(18).
51. Zhang L, Zheng Y, Zeng L, et al. 3-Epipachysamine B suppresses proliferation and induces apoptosis of breast cancer cell via PI3K/AKT/mTOR signaling pathway[J]. *Life Sci*. 2021;285:119995.
52. Zhao XY, Yang YY, Feng JL et al. Network Pharmacology Prediction and Experimental Validation of *Trichosanthes-Fritillaria thunbergii* action mechanism against Lung Adenocarcinoma[J]. *J Vis Exp*, 2023, (193).
53. Guo J, Zhao Y, Wu X, et al. Mechanism exploration and prognosis study of *Astragal Radix*-spreading hedyotis herb for the treatment of lung adenocarcinoma based on bioinformatics approaches and molecular dynamics simulation[J]. *Front Chem*. 2023;11:1128671.
54. Qi YS, Xie JB, Xie P, et al. Uncovering the anti-NSCLC effects and mechanisms of gypenosides by metabolomics and network pharmacology analysis[J]. *J Ethnopharmacol*. 2021;281:114506.
55. Lin Z, Zhang Z, Ye X, et al. Based on network pharmacology and molecular docking to predict the mechanism of Huangqi in the treatment of castration-resistant prostate cancer[J]. *PLoS ONE*. 2022;17(5):e0263291.

56. Sun Y, Liu Y, Ma X et al. The influence of cell cycle regulation on Chemotherapy[J]. *Int J Mol Sci*. 2021, 22(13).
57. Kong Y, Allison DB. The kinase PLK1 promotes the development of Kras/Tp53-mutant lung adenocarcinoma through transcriptional activation of the receptor RET[J]. 2022, 15(754): eabj4009.
58. Zhang P, Zhang X, Zhu Y, et al. Polo-like kinase 1 suppresses lung adenocarcinoma immunity through necroptosis[J]. *Oncol Res*. 2023;31(6):937–53.
59. Malumbres M. Cyclin-dependent kinases[J]. *Genome Biol*. 2014;15(6):122.
60. Yang L, Xiong H, Li X, et al. Network Pharmacology and comparative transcriptome reveals biotargets and mechanisms of Curcumol treating lung adenocarcinoma patients with COVID-19[J]. *Front Nutr*. 2022;9:870370.
61. Li S, Li H, Cao Y et al. Integrated bioinformatics analysis reveals CDK1 and PLK1 as potential therapeutic targets of lung adenocarcinoma[J]. 2021, 100(32): e26474.
62. Dai Y, Grant S. New insights into checkpoint kinase 1 in the DNA damage response signaling network[J]. *Clin Cancer Res*. 2010;16(2):376–83.
63. Grabauskiene S, Bergeron EJ, Chen G, et al. CHK1 levels correlate with sensitization to pemetrexed by CHK1 inhibitors in non-small cell lung cancer cells[J]. *Lung Cancer*. 2013;82(3):477–84.
64. Cai K, Xie Z, Liu Y et al. Identification of Potential Key Genes and Prognostic Biomarkers of Lung Cancer Based on Bioinformatics[J]. 2023, 2023: 2152432.
65. Tan Z, Chen M, Wang Y, et al. CHEK1: a hub gene related to poor prognosis for lung adenocarcinoma[J]. *Biomark Med*. 2022;16(2):83–100.
66. Li Z, Yu B, Qi F, et al. KIF11 serves as an independent prognostic factor and therapeutic target for patients with lung Adenocarcinoma[J]. *Front Oncol*. 2021;11:670218.
67. Zheng L, Chen Z, Kawakami M et al. Tyrosine threonine kinase inhibition eliminates lung cancers by augmenting apoptosis and Polyploidy[J]. 2019, 18(10): 1775–86.
68. Chen X, Yu C, Gao J, et al. A novel USP9X substrate TTK contributes to tumorigenesis in non-small-cell lung cancer[J]. *Theranostics*. 2018;8(9):2348–60.
69. Li B, Gu X. Comprehensive analysis of the prognostic value and immune implications of the TTK gene in lung adenocarcinoma: a meta-analysis and bioinformatics analysis[J]. 2022, 26(3): 108–18.

Publisher's Note

Springer Nature remains neutral with regard to jurisdictional claims in published maps and institutional affiliations.